Synergistic Inhibitor Binding to *Streptococcus pneumoniae* 5-Enolpyruvylshikimate-3-phosphate Synthase with Both Monovalent Cations and Substrate

Wensheng Du,[‡,§] Wu-Schyong Liu,[||] David J. Payne,*[,‡] and Michael L. Doyle*[,⊥,#]

Department of Anti-Infectives Research, SmithKline Beecham Pharmaceuticals, 1250 South Collegeville Road, Collegeville, Pennsylvania 19426, and Departments of Structural Biology and Protein Biochemistry, SmithKline Beecham Pharmaceuticals, 709 Swedeland Road, King of Prussia, Pennsylvania 19406

Received April 19, 2000

ABSTRACT: The inhibitor binding synergy mechanism of the bi-substrate enzyme *Streptococcus pneumoniae* 5-enolpyruvylshikimate-3-phosphate synthase (EPSPS) has been investigated with a linkage thermodynamics strategy, involving direct binding experiments of one ligand conducted over a range of concentration of the other. The results demonstrate that binding of the inhibitor glyphosate (GLP) is highly synergistic with both a natural substrate shikimate-3-phosphate (S3P) and activating monovalent cations. The synergy between GLP and S3P binding was determined to be 1600-fold and is in qualitative agreement with previous work on *Escherichia coli* EPSPS. The binding molar ratios of S3P and GLP were measured as 1.0 and 0.7 per EPSPS, respectively. Monovalent cations that have been shown previously to stimulate *S. pneumoniae* EPSPS catalytic activity and its inhibition by GLP were found here to exhibit a similar rank-order with respect to their measured GLP binding synergies (ranging from 0 to ≥3000-fold increase in GLP affinity). The cation specificity and the sub-millimolar concentrations where these effects occur strongly suggest the presence of a specific cation binding site. Analytical ultracentrifugation data ruled out GLP-binding synergy mechanisms that derive from, or are influenced by, changes in oligomerization of *S. pneumoniae* EPSPS. Rather, the data are most consistent with an allosteric mechanism involving changes in tertiary structure. The results provide a quantitative framework for understanding the inhibitor binding synergies in *S. pneumoniae* EPSPS and implicate the presence of a specific cation binding regulatory site. The findings will help to guide rational design of novel antibiotics targeting bacterial EPSPS enzymes.

5-Enolpyruvylshikimate-3-phosphate (EPSP)[1] synthase (EPSPS, EC 2.5.1.19) catalyzes the penultimate step in the prechorismate part of the shikimate pathway (*1*). The reaction involves a freely reversible transfer of an enolpyruvyl group from phosphoenol pyruvate (PEP) to shikimate 3-phosphate (S3P) to yield 5-enolpyruvylshikimate-3-phosphate (EPSP) and inorganic phosphate (Pi). The only other enzyme known to catalyze this type of enolpyruvyl group transfer is UDP-*N*-acetylglucosamine enolpyruvyl transferase (MurA), which catalyzes the first committed step in bacterial cell wall biosynthesis (*2*).

Interest in the inhibition mechanism of EPSPS initially came from the fact that EPSPS is the target for the widely used, broad-spectrum herbicide glyphosate (*N*-phosphonomethylglycine, GLP) (*3*). Early work suggested that GLP inhibits EPSPS by functioning as a transition-state analogue of PEP (*4*) and was supported by evidence with the *Escherichia coli* enzyme from enzyme kinetics (*5*), equilibrium fluorescence titration (*6*), solid-state NMR (*7*), and differential scanning calorimetry (*8*). These studies demonstrated that GLP preferentially forms a ternary complex with enzyme and S3P (EPSPS·S3P·GLP), and there is overlap between the PEP and GLP binding sites. However, more recent experiments by steady-state kinetics (*9*), analysis of synthetic analogues of the EPSPS·S3P·GLP ternary complex (*10, 11*), and site-directed mutagenesis of putative active site residues (*12*−*14*) indicate that GLP is not exactly superimposable with PEP when S3P is present, and there is no clear correlation between the inhibition by GLP and catalytic efficiency at the PEP site. Consequently, GLP is believed to be an adventitious allosteric effector that competes with PEP binding indirectly through conformational change in EPSPS (*15*). Nevertheless, the ternary complex EPSPS·S3P·GLP is generally believed to be responsible for GLP's herbicidal activity (*15*). Interestingly, there is a strong synergy (80000-fold) between binding of GLP and S3P to

* To whom correspondence should be addressed. E-mails: Michael.Doyle@bms.com and David_J_Payne@sbphrd.com.

‡ Department of Anti-Infectives Research.

§ Present address: Lead Discovery, Bristol-Myers Squibb Pharmaceutical Research Institute, 5 Research Parkway, Wallingford, CT 06492.

|| Protein Biochemistry.

⊥ Structural Biology.

Present address: Biopharmaceuticals Department, Bristol-Myers Squibb Research Institute, Princeton, NJ 08543-4000.

[1] Abbreviations: EPSP, 5-enolpyruvylshikimate-3-phosphate; EPSPS, 5-enolpyruvylshikimate-3-phosphate synthase; GLP, glyphosate; Hepes, *N*-[2-hydroxyethyl]piperazine]-*N*′-[2-ethanesulfonic acid]; ITC, isothermal titration calorimetry; MALDI-TOF, matrix-assisted laser desorption/ionization time-of-flight; MurA, UDP-*N*-acetylglucosamine enolpyruvyl transferase; PEP, phospho(enol)pyruvate; S3P, shikimate 3-phosphate; UDPNAG, UDP-*N*-acetylglucosamine.

10.1021/bi000890v CCC: $19.00
Published on Web 07/27/2000

the *E. coli* EPSPS enzyme (*16*). The synergy mechanism was also attributed to GLP-induced stabilization of the "closed" conformation of EPSPS·S3P. This conclusion is supported in part by limited tryptic digestion and MALDI-TOF mass spectrometry studies on EPSPS carried out in parallel with studies on the homologous model system MurA, for which both open and closed crystal structures have been solved (*17*). Thus far only the "open" conformation crystal structure of EPSPS has been reported (*18*).

Current interest in the inhibition mechanism of EPSPS is stimulated by its potential as a broad-spectrum, novel antibacterial target. We have previously reported the cloning, overexpression, purification, and initial enzymological characterization of EPSPS from the Gram positive pathogen *Streptococcus pneumoniae* (*19*). We found that the catalytic activity of *S. pneumoniae* EPSPS was enhanced by specific monovalent cations (e.g., NH_4^+ and K^+) and that its inhibition by GLP was also substantially increased by NH_4^+ (*19*). Monovalent cations have also been reported to modulate *Bacillus subtilis* EPSPS (*20*), and ammonium and GLP were proposed to regulate the oligomeric state of *B. subtilis* EPSPS (*14*).

Here we have investigated the GLP inhibition mechanism of *S. pneumoniae* EPSPS, and its synergistic interactions with substrate S3P and monovalent cations using direct biophysical approaches. We utilized a linkage thermodynamics method to determine binding and synergy interaction energies, based on calorimetric GLP titrations of EPSPS as a function of substrate and vice-a-versa. Similar experiments were done with GLP and monovalent cations. The monovalent cations investigated include the best reported activator (NH_4^+), a moderate activator (K^+), and a nonactivator (Cs^+) of EPSPS (*19*). Additionally, we conducted analytical ultracentrifugation and circular dichroism experiments to examine whether the observed synergy effects are the result of changes in oligomerization or secondary structure change. The findings help to deconvolute the synergistic inhibition mechanism of EPSPS, and also reveal the critical role that monovalent cations play.

EXPERIMENTAL PROCEDURES

Chemicals and Enzyme. Chemicals were from Sigma. S3P and the *S. pneumoniae* EPSPS were prepared as described previously (*19*). Hepes buffer (5 mM, pH 7.0) was used in all experiments, and the pH of the solutions was adjusted by tetramethylammonium hydroxide. EPSPS was dialyzed extensively against buffer prior to each experiment.

Isothermal Titration Calorimetry (ITC). Measurements were made with either MCS or VP−ITC instruments (MicroCal, Inc. Northampton, MA) (*21*, *22*). Dialyzed enzyme and pH-adjusted ligand solutions were degassed for 10 min prior to each titration. EPSPS molarity was determined by absorbance at 280 nm using an extinction coefficient of 10 950 M^{-1} calculated from sequence (*23*). Titrant concentrations were determined gravimetrically. For titrations of one ligand carried-out over a range of a second ligand, the second ligand was added to a concentration in excess over EPSPS so that its activity would be essentially constant over the course of the titration. Titrations were carried out with injection volumes of 5−10 μL and a time interval between injections of 200 s. A preliminary injection of 2 μL was made before each titration to ensure the titrant concentration was at its loading value. Binding isotherms were fitted by nonlinear regression using the 1:1 stoichiometric model provided in the Origin ITC software (MicroCal, Inc.) (*21*). The binding molar ratio (N), association constant (K_a), and enthalpy change (ΔH) were floating parameters for all titrations. Equilibrium dissociation constants (K_d) were calculated as the reciprocal of the binding association constant. Regression analyses of the functional dependence of binding constants on concentration of second ligands or salt activity was done with GraFit υ4.09 (Erithacus Software Ltd.) or SigmaPlot, version 5.0 (SPSS, Inc.) software.

Analytical Ultracentrifugation. Sedimentation equilibrium data were measured on a Beckman XL-A analytical ultracentrifuge. Samples were loaded in double sector cells with charcoal filled Epon centerpieces and sapphire windows. The data were analyzed with a single, homogeneous species model as (*24*)

$$c_r = c_m \exp\left[\frac{M(1-\bar{\nu}\rho)\omega^2(r^2 - r_m{}^2)}{2RT}\right] + \text{base} \qquad (1)$$

where c_m and c_r are the enzyme concentrations at the meniscus reference radial position and as a function of radial position r, respectively, and base is a baseline absorbance that is constant as a function of radial position. M is the solution mass of the enzyme, $\bar{\nu}$ is the partial specific volume of the enzyme, ρ is the solvent density, ω is the angular velocity in radians per second, r is the radial position, r_m is the radial position of the meniscus, R is the gas constant, and T is absolute temperature. In the conditions of the present study the solution density ranged from $\rho = 1.000-1.011$ g/mL, depending on type and concentration of salt used, and $\bar{\nu}$ was calculated from the sequence as 0.7488 mL/gm. The floating parameters in eq 1 are M, c_m, and base. EPSPS (initially at 1.26 mg/mL) was analyzed under each of the conditions listed in Table 3 with the corresponding reference solution containing all the components except the enzyme.

Circular Dichroism. Circular dichroism spectra were measured on a Jasco J-710 CD Spectropolarimeter at 0.3 mg/mL EPSPS with 0.5 M NH_4Cl in a 0.1 cm path length water-jacketed cuvette at 20 °C. Wavelength scans were made at 50 nm/min and 4 spectra were averaged in each case. Raw ellipticity data, θ (millidegrees), were converted to molar difference extinction coefficient units, $\Delta\epsilon$, by the relation $\Delta\epsilon = \theta/(32.98 \times l \times c \times 1000)$ (*25*), where l is the path length in centimeters and c is the EPSPS molarity normalized to units of amino acid residues. Concentration of EPSPS was determined by absorbance at 280 nm using an extinction coefficient of 0.239 mL/mg as calculated from sequence (*23*). Thermal stability curves were measured by scanning temperature at 1 °C/min. The temperature at which the protein was half-unfolded (T_m) was approximated graphically as the temperature at the midpoint of the transition in ellipticity.

RESULTS

Binding Synergy between GLP and S3P. In the present study we carried out direct binding measurements of GLP and S3P to *S. pneumoniae* EPSPS using titration calorimetry. Figure 1 shows data for titrating EPSPS with GLP in the

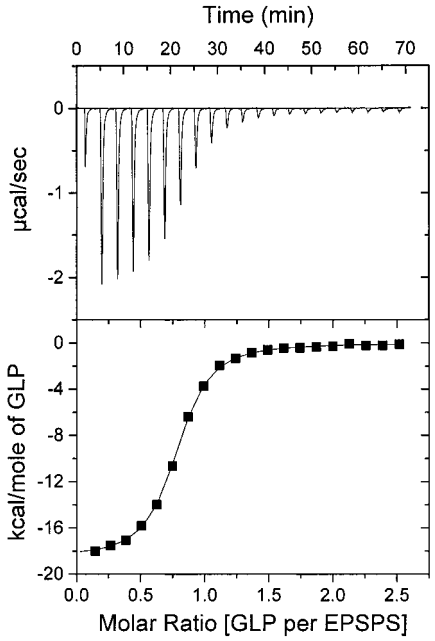

FIGURE 1: Isothermal titration calorimetry data for the titration of *S. pneumoniae* EPSPS with GLP. EPSPS was titrated with 5 μL injections of 0.4 mM GLP. Top: raw data as microcalories per second. Bottom: amount of heat measured per mole of GLP injected versus accumulated molar ratio of GLP added per EPSPS in the cell. Solid curve is the best-fit for a single binding site model. Best-fit parameters were $^{GLP}K_{d,obs} = 4\ (\pm 0.2) \times 10^{-7}$ M, $\Delta H = -18.2$ ($\pm$0.1) kcal/mol, and molar ratio = 0.745 ($\pm$0.004). Conditions: 20 μM EPSPS, 5 mM Hepes, 500 mM NH_4Cl, 1 mM S3P, pH 7.0, and 25 °C.

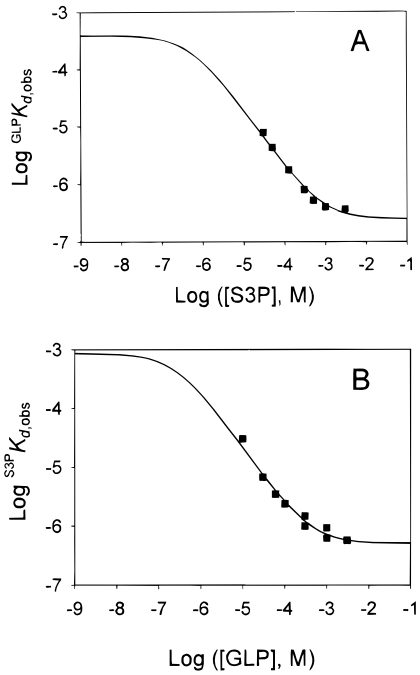

FIGURE 2: (A) S3P dependence of GLP affinity to EPSPS shown as logarithm of the observed equilibrium dissociation constant for GLP binding versus logarithm of the molarity of S3P concentration. Best-fit curve represents a thermodynamic linkage model for single-site binding of both GLP and S3P to EPSPS (eq 2). Best-fit parameters are $^{GLP}K_{d,1} = 0.25\ (\pm 0.05)\ \mu$M and $^{S3P}K_{d,0} = 770\ (\pm 290)\ \mu$M. (B) GLP dependence of S3P binding to EPSPS. Best-fit curve is analogous to eq 2. Best-fit parameters are $^{S3P}K_{d,1} = 0.51\ (\pm 0.09)\ \mu$M and $^{GLP}K_{d,0} = 420\ (\pm 100)\ \mu$M. Conditions: 5−20 μM EPSPS, 5 mM Hepes, 500 mM NH_4Cl, pH 7.0, and 25 °C.

presence of saturating S3P. The observed GLP-binding molar ratio was found to be 0.7 $\pm$ 0.05 per EPSPS which is close to the theoretical value expected for a 1:1 stoichiometry. Similarly, the molar ratio for binding of S3P to EPSPS was found to be 1.0 $\pm$ 0.1.

To determine the GLP affinity for the EPSPS·S3P complex, we measured GLP binding calorimetry data over a range of S3P concentration. This approach provides a more comprehensive evaluation of the binding synergy model between GLP and S3P than is possible with a single titration measured at a high, saturating concentration. It also allows determination of weak binding constants, which might otherwise require prohibitively high concentrations of reagents. Figure 2A summarizes these titrations as the logarithm of the observed GLP dissociation constant versus total concentration of S3P. The S3P dependence of the observed GLP dissociation constant $^{GLP}K_{d,obs}$ is given by the following three-parameter thermodynamic linkage equation (*26*, *27*):

$$\log {}^{GLP}K_{d,obs} = \log {}^{GLP}K_{d,0} + \log\left[\frac{1 + \frac{[S3P]}{{}^{S3P}K_{d,0}}}{1 + \frac{[S3P]}{{}^{S3P}K_{d,1}}}\right] \quad (2a)$$

Here $^{GLP}K_{d,0}$ is the GLP dissociation constant in the absence of S3P, [S3P] is the unbound concentration of S3P (approximated by the total [S3P] for the case of [S3P] > [EPSPS]), and $^{S3P}K_{d,0}$ and $^{S3P}K_{d,1}$ are the S3P dissociation constants in the absence of GLP and to the EPSPS·GLP complex, respectively. As can be seen in Figure 2A, the data

Scheme 1: Thermodynamic Cycle Describing the Linkage between Binding of S3P and GLP to EPSPS. Equilibrium Dissociation Constants Are Defined Right to Left for S3P Interactions, and Bottom to Top for GLP Interactions.

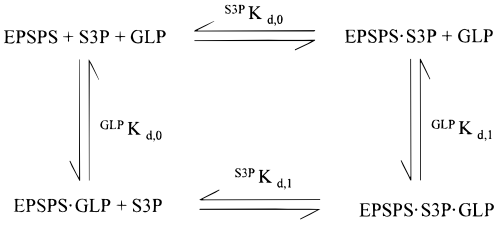

were measured primarily at the high-concentration asymptote and thus only provide partial information about the linkage between GLP and S3P binding. To fit the data to a form of linkage eq 2 that is more appropriate for the information content of the data, we exploited the conservation of energy relationship between parameters (Scheme 1) and reparametrized eq 2 to allow fitting directly for the parameters $^{GLP}K_{d,1}$, the GLP dissociation constant of the EPSPS·S3P complex, and $^{S3P}K_{d,0}$. Substituting $^{GLP}K_{d,0} = {}^{S3P}K_{d,0}{}^{GLP}K_{d,1}/{}^{S3P}K_{d,1}$ into eq 2a gives the fitting equation used in Figure 2A:

$$\log {}^{GLP}K_{d,obs} = \log\left[\frac{{}^{S3P}K_{d,0}\,{}^{GLP}K_{d,1}}{{}^{S3P}K_{d,1}}\right] + \log\left[\frac{1 + \frac{[S3P]}{{}^{S3P}K_{d,0}}}{1 + \frac{[S3P]}{{}^{S3P}K_{d,1}}}\right] \quad (2b)$$

Table 1: Equilibrium Dissociation Constants for the Synergistic Linkage between GLP and S3P Binding to EPSPS[a]

parameter	K_d (μM)
$^{GLP}K_{d,0}$	420 (±100)
$^{GLP}K_{d,1}$	0.25 (±0.05)
$^{S3P}K_{d,0}$	770 (±290)
$^{S3P}K_{d,1}$	0.51 (±0.09)

[a] Parameters are defined in Scheme 1. Conditions: 5 mM Hepes, 500 mM NH_4Cl, pH 7.0, and 25 °C.

The high-concentration asymptote of the function yields $^{GLP}K_{d,1}$, and the curvature approaching that asymptote defines the parameter $^{S3P}K_{d,0}$. The remaining parameter, $^{S3P}K_{d,1}$, which is given by the curvature approaching the low-concentration asymptote in Figure 2A, cannot be determined due to lack of data in that region of the function and had to be constrained to the value measured from the high-concentration asymptote of the complementary dataset in Figure 2B. Even so, the magnitude of the observed decrease in $^{GLP}K_{d,obs}$ does partially define $^{S3P}K_{d,1}$ by setting a minimum magnitude to the overall synergy. During regression analysis of the data in Figure 2A (eq 2b) we found the value of $^{S3P}K_{d,1}$ could be constrained to any value less than 10^{-5} M without altering the best-fit values of the remaining fitting parameters $^{GLP}K_{d,1}$ and $^{S3P}K_{d,0}$. The actual value it was constrained to, 5×10^{-7} M, was determined independently from the data in Figure 2B.

The data in Figure 2B were analyzed using an equation analogous to eq 2b that describes the GLP dependence of the S3P affinity of EPSPS. To resolve all parameters in Scheme 1 it was necessary to analyze both sets of data in Figure 2, panels A and B. The results from both analyses are summarized in Table 1. The binding synergy between GLP and S3P can be calculated as the ratio of dissociation constants on parallel sides of the thermodynamic cycle of Scheme 1, as $^{GLP}K_{d,0}/^{GLP}K_{d,1} = 1680$ and $^{S3P}K_{d,0}/^{S3P}K_{d,1} = 1540$. The agreement between these two ratios serves as a touchstone to affirm that the simple binding model used for the two independent sets of data is correct.

Binding Synergy between GLP and Monovalent Cations. Previously we showed by enzyme kinetics methods that inhibition of *S. pneumoniae* EPSPS with GLP is enhanced in the presence of specific monovalent cations (*19*). Here we have measured directly the thermodynamic coupling between binding GLP and monovalent cations using titration calorimetry. Titrations were conducted at a constant concentration of S3P in far excess over the EPSPS concentration, and where EPSPS is largely S3P-bound. Previous work has shown the S3P binding K_m of *S. pneumoniae* EPSPS is only slightly sensitive to salt activities from 1 to 100 mM (*19*). Figure 3 shows GLP binding constants of EPSPS as a function of varying activities of NH_4Cl, KCl, or CsCl. At activities between 0.1 and 100 mM, ammonium ion is seen to increase the GLP affinity of EPSPS·S3P complex by 2 orders of magnitude. Potassium has about a 1 order of magnitude effect on GLP affinity, and cesium has practically no effect. The striking differences observed for these cations, together with the fact that they are observed at low salt concentrations where generic ionic strength effects are minimal, strongly suggests that a specific cation binding site is involved. In contrast, at high salt activities where ionic strength changes are likely to exist, all three cations exhibit

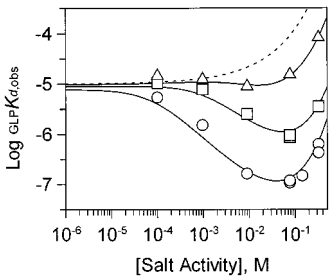

FIGURE 3: Salt dependence of the observed equilibrium dissociation constant for GLP binding to EPSPS versus activity of various monovalent cation chloride salts: NH_4Cl (○), KCl (□), and CsCl (△). GLP binding constants were measured by ITC. Salt activities were calculated from total concentrations with activity coefficients (*43*). Solid curves are the best fits of the data to eq 3. Best-fit parameters are in Table 2. Dotted curve shows the predicted influence from nonspecific ionic strength effects (eq 3). Conditions: 5−20 μM EPSPS, 5 mM Hepes, 1 mM S3P, pH 7.0, and 25 °C.

a similar 1 order of magnitude reduction in GLP affinity. The data in Figure 3 were fitted to the simplest model reasonable for describing the biphasic salt dependencies:

$$\log {}^{GLP}K_{d,obs} = \log {}^{GLP}K_{d,0,S3P} + \log\left[\frac{1 + \frac{a_{salt}}{{}^{cation}K_{d,0}}}{1 + \frac{a_{salt}}{{}^{cation}K_{d,1}}}\right] - A\sqrt{a_{salt}} \quad (3)$$

Here $^{GLP}K_{d,0,S3P}$ is the GLP dissociation constant of the EPSPS·S3P complex at zero salt activity, $^{cation}K_{d,0}$ and $^{cation}K_{d,1}$ are cation dissociation constants in the unbound and GLP-bound forms of EPSPS·S3P, a_{salt} is the salt activity, and A is an empirical constant. The first two terms on the right-hand side of eq 3 represent a standard thermodynamic linkage relationship between two different ligands (*27*, *28*). The third term on the right-hand side is the simplest empirical function we found that was sufficient to describe the effects at high salt activities for all cations. This latter empirical term is not intended to convey molecular meaning, but does, perhaps coincidentally, resemble the Debye−Huckel limiting law for ionic strength nonideality effects (*29*). The dotted curve in Figure 3 represents the deconvoluted contribution from this term. It can be seen to have minimal influence on the overall fitting function up to about 10 mM salt activity. At higher salt activity, it makes a significant contribution and may partially obscure resolution of the specific cation binding linkage parameter $^{cation}K_{d,0}$. The results for unconstrained fitting of the data to eq 3 are given in Table 2. All parameters are well resolved except for $^{cation}K_{d,0}$. This parameter is determined from data at the higher salt activities and is numerically correlated with the parameter A. Nevertheless, the values reported in Table 2 give the minimum synergy factor between GLP and cation binding. The difference in binding affinity of ammonium for the unbound and GLP-bound enzyme is estimated to be at least 3000-fold. This difference is reduced to only 300-fold for potassium and is negligibly small for cesium. These results demonstrate that ammonium has a strong binding synergy with GLP, and the selectivity between monovalent cation type strongly suggests

Table 2: Equilibrium Dissociation Constants for the Synergistic Linkage between GLP and Monovalent Cation Binding to EPSPS.[a]

salt	$^{GLP}K_{d0,S3P}$ (mM)	$^{cation}K_{d0}$ (mM)	$^{cation}K_{d1}$ (mM)	A
NH_4Cl	0.0074 (±0.0022)	300 (±330)	0.095 (±0.034)	−3.9 (±0.43)
KCl	0.0088 (±0.0018)	270 (±230)	1.1 (±0.32)	−3.2 (±0.33)
CsCl	0.0097 (±0.0028)	nd	nd	−3.0 (±1.6)

[a] Standard errors for unconstrained fitting are listed. Conditions: 5 mM Hepes, 1 mM S3P, pH 7.0 and 25 °C. nd is not determined due to undetectable linkage effect.

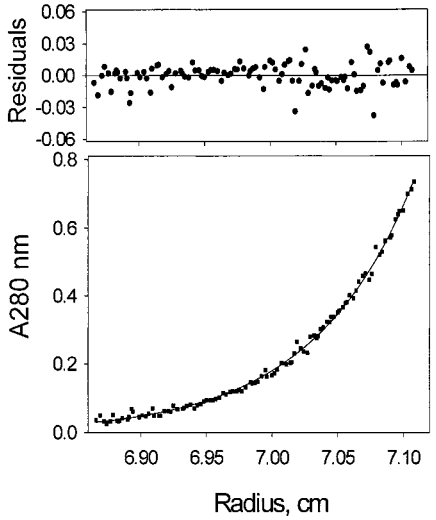

FIGURE 4: Sedimentation equilibrium data for EPSPS. Lower: Absorbance at 280 nm versus radial position. Data points are shown with the best-fit curve for a single-species model (eq 1). Best-fit weight-average molecular mass is M_w = 45.0 (±0.7) kDa and indicates EPSPS (45.8 kDa by mass spectrometry) is monomeric. Upper: Residuals for the best fit. Conditions: 5 mM Hepes, 100 mM NH_4Cl, pH 7.0, 20 °C, and 19 000 rpm.

a specific binding site is involved (*30*). In fact, under physiological concentrations of ammonium (*31*), GLP binding may be a prerequisite to ammonium binding at the cation synergy site. While the number of cation binding sites cannot be conclusively determined from the data in Figure 3, the best-fit curves are consistent with an independent and identical binding site model (*27*).

Monomeric State of EPSPS. We also evaluated by analytical ultracentrifugation whether the observed synergy for ligand binding in EPSPS is due to an oligomerization mechanism. Previous work on *B. subtilis* EPSPS indicated that it can exist as monomer, dimer, and tetramer oligomeric forms in a manner dependent on various ligands (*14*). We therefore measured the molecular weight of *S. pneumoniae* EPSPS by sedimentation equilibrium in the presence of various combinations of S3P, GLP, and monovalent cations. The monovalent cations include the best reported activator (NH_4^+), a moderate activator (K^+), and a nonactivator (Cs^+) of EPSPS (*19*). A sample sedimentation equilibrium data set is shown in Figure 4. Best-fit weight-average molecular weights are listed in Table 3 and are similar to the monomer molecular weight measured by MALDI mass spectroscopy (45 800) and predicted from sequence (45 800). Moreover, the data for all conditions were very well described by a homogeneous species model (eq 1) as judged by random residuals (Figure 4). These results demonstrate that *S. pneumoniae* EPSPS does not appreciably oligomerize at concentrations up to approximately 100 μM (concentration near 1 absorbance unit at 280 nm). However, we note that the weight-average molecular weight in the 1 mM S3P plus

Table 3: Weight-Average Molecular Weights of *S. pneumoniae* EPSPS in the Presence or Absence of Ligands and Monovalent Cations Measured by Sedimentation Equilibrium at pH 7.0 and 20 °C

condition	M_w (kDa)
no ligands	43.3 ± 0.8
1 mM S3P	46.1 ± 0.3
50 mM GLP	43.3 ± 0.6
1 mM S3P + 100 mM NH_4Cl	52.4 ± 0.3
1 mM S3P + 100 mM NH_4Cl + 4 mM GLP	51.1 ± 0.2
10 mM NH_4Cl	42.5 ± 0.7
100 mM NH_4Cl	45.0 ± 0.7
500 mM NH_4Cl	44.9 ± 0.4
100 mM KCl	44.8 ± 0.4
100 mM CsCl	45.5 ± 0.4

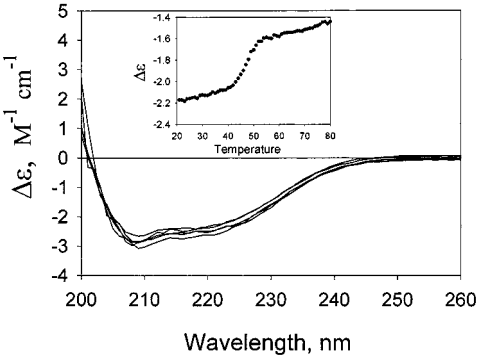

FIGURE 5: Circular dichroism spectra of EPSPS in the presence or absence of various ligands. Molar difference extinction coefficient is shown versus wavelength for EPSPS under various ligand conditions. Conditions: 5 mM Hepes, 500 mM NH_4Cl, and pH 7.0 with no ligand, 1 mM PEP, 1 mM S3P, 1 mM GLP, and 1 mM S3P plus 1 mM GLP. Inset: Thermal stability of EPSPS monitored by ellipticity at 222 nm. Unfolding midpoint T_m is 47 °C.

100 mM NH_4Cl condition (52 400) is somewhat larger than expected for a pure monomer. We constrained the fit of the data for these conditions to a monomer−dimer model (*24*) and predicted a very weak dimerization constant equal to 480 μM. Thus, it is possible that a small amount of oligomerization occurs at high concentrations. Nevertheless, it is important to note that at the low concentrations of EPSPS studied herein by calorimetry (5−20 μM) and CD spectroscopy (7 μM) the possible influence of dimer species is negligible (<4% as dimer).

Secondary Structure and Thermal Stability Analysis. We measured the CD spectra of EPSPS in the presence and absence of various combinations of ligands to evaluate whether the synergy mechanism involves substantial changes in secondary structure folding. Figure 5 shows the CD spectra under all the conditions studied, and indicates there are no detectable changes in CD spectrum with ligands. This indicates that the binding synergy is unlikely to involve large (>20%) changes in secondary structure.

We also measured the thermal stability of EPSPS by circular dichroism in order to establish the maximum

experimental temperature for the present studies. We found that the unfolding midpoint, T_m, for EPSPS is 47 °C and is somewhat low relative to typical protein unfolding midpoints of 60 °C (*32*). The data in the inset to Figure 5 indicate that EPSPS remains in its native form up to about 35−40 °C.

DISCUSSION

Inhibitor−Substrate Binding Synergy. The present calorimetry study reveals a large, 1600-fold synergy between binding of inhibitor GLP and substrate S3P to *S. pneumoniae* EPSPS. Similar observations have been made for *E. coli* EPSPS using calorimetric (*16*) and steady-state enzymological methods (*33*), although the synergy factor was somewhat larger (80000-fold). The lower synergy observed for *S. pneumoniae* EPSPS originates almost entirely from its 30-fold higher affinity for GLP in the absence of S3P ($^{GLP}K_{d,0}$ = 420 and 12 000 μM for *S. pneumoniae* and *E. coli* EPSPS, respectively). Both enzymes bind GLP with similar affinity in their S3P-bound forms ($^{GLP}K_{d,1}$ = 0.25 and 0.15 μM for *S. pneumoniae* and *E. coli* EPSPS−S3P, respectively). On the other hand, the S3P affinity of *S. pneumoniae* EPSPS in the absence of GLP is 70-fold weaker than that of *E. coli* EPSPS ($^{S3P}K_{d,0}$ = 720 and 10 μM for *S. pneumoniae* and *E. coli* EPSPS, respectively). The S3P affinity for the GLP-bound form of *E. coli* EPSPS has not been measured, but is predicted from conservation of energy (Scheme 1) to be 4000-fold tighter than that of *S. pneumoniae* EPSPS. The differences in the binding affinities and synergies between *S. pneumoniae* and *E. coli* forms of EPSPS are not surprising, due to their low, 25% sequence identity (*19*). Additionally, as discussed below, differences in solution conditions, such as concentration and type of monovalent cation, can substantially alter S3P and GLP binding properties of *S. pneumoniae* EPSPS.

Comparison of the direct binding parameters measured in this study (Table 1) to those obtained under very similar conditions with the *S. pneumoniae* EPSPS enzyme by steady-state enzyme kinetics methods (*19*) reveals features that are reminiscent of those reported for *E. coli* EPSPS (*16*, *33*). The equilibrium dissociation constant for binding GLP to the *S. pneumoniae* EPSPS·S3P complex ($^{GLP}K_{d,1}$ = 0.25 μM) agrees very well with the inhibition constant (K_i = 0.3 μM, competitive model with respect to PEP) obtained under similar conditions (saturating S3P) (*19*). However, the S3P affinity of the EPSPS·GLP complex ($^{S3P}K_{d,1}$ = 0.51 μM) is 60-fold tighter than the analogous interaction with EPSPS·PEP that was determined kinetically [K_m(S3P) = 31 μM] (*19*). This demonstrates that the S3P binding synergy is greater with the inhibitor GLP than with the physiological substrate PEP, and agrees qualitatively with results on the *E. coli* EPSPS (*16*, *33*). The PEP affinity for EPSPS·S3P determined kinetically [K_m(PEP) = 22 μM] (*19*) is 90-fold weaker than the GLP affinity for EPSPS·S3P ($^{GLP}K_{d,1}$ = 0.25 μM), and also agrees qualitatively with results on the *E. coli* enzyme.

The synergistic inhibition mechanism of *S. pneumoniae* EPSPS most likely involves a sizable conformational change. Previous studies on *E. coli* EPSPS (reviewed in ref *15*) implicate GLP synergy may stem from allosteric means. This fits in well with expectations from structural studies on EPSPS and its structural homologue MurA, a closely related enolpyruvyl transferase. The unliganded forms of both enzymes exist in a two-domain "open" conformation (*18*, *34*). Upon binding substrate (UDP-*N*-acetylglucosamine, UDPNAG) and inhibitor (fosfomycin) MurA has been shown to undergo a dramatic change in tertiary structure to a "closed" form, in which the two domains rearrange into a tightly packed conformation (*35*). Three-dimensional structural information on a ligand-bound form of EPSPS has not yet been reported. However, by using limited tryptic digestion and MALDI-TOF mass spectrometry, Krekel et al. (*17*) analyzed substrate and inhibitor-induced conformational changes of both *Enterobacter cloacae* MurA and *E. coli* EPSPS. Their results indicate that S3P in combination with GLP stabilizes EPSPS to a "closed" conformation.

The present study on *S. pneumoniae* EPSPS is also consistent with an "open-closed" tertiary structure change allosteric model for several reasons. The circular dichroism results indicate changes in secondary structure are minimal, so that large changes in folding are unlikely. Analytical ultracentrifugation results indicate changes in quaternary structure are absent at EPSPS concentrations below 100 μM, and rule out oligomerization synergy mechanisms. Also, the buffer ionization-corrected (*36*) GLP binding enthalpy change we observe (−18 kcal/mol with saturating S3P) is similar to that observed for *E. coli* EPSPS (*16*) and is somewhat large for a small molecule-protein interaction. This may reflect enthalpy changes that accompany tertiary conformational changes. Interestingly, the observed S3P binding enthalpy change is much smaller (−3 kcal/mol in saturating GLP). These thermodynamic trends (*37*) are consistent with GLP alone being sufficient to drive an open-closed conformational transition, whereas S3P alone does not appear to be sufficient. This situation is somewhat different than that for *E. coli* EPSPS, where the presence of both S3P and GLP was required to induce protection against proteolysis (*17*).

Monovalent Cation−Inhibitor Binding Synergy. Certain monovalent cations play a substantial role in increasing the GLP affinity of *S. pneumoniae* EPSPS. We find here that 100 mM NH_4Cl causes an almost two-orders of magnitude increase in the GLP affinity of the EPSPS·S3P complex (Figure 3). Previous steady-state enzyme kinetics studies under similar conditions with *S. pneumoniae* EPSPS also showed certain monovalent cations increase the inhibition affinity of GLP and activate enzyme activity (*19*). Additionally, ammonium enhancement of catalysis and GLP inhibition of *B. subtilis* EPSPS has been reported (*14*, *20*). As pointed out previously (*20*), the rank-order effectiveness of monovalent cations causing these synergistic effects correlates to their unhydrated radii, with ammonium having the greatest effect. The stereoselectivity of these effects suggests a specific binding pocket for monovalent cations (*30*) exists on these bacterial species of EPSPS, presumably formed by amino acid residues bearing electronegative acceptor atoms (*38*, *39*). Additional evidence for a specific monovalent cation binding site on EPSPS comes from the results in Figure 3, which show that the differential effects of the cations are pronounced at low salt activities (0.1−100 mM) where nonspecific ionic strength effects are minimal. In contrast, at higher salt activities (>100 mM) all three cations exhibit a similar reduction in GLP affinity. These high salt effects are probably due to a combination of both electrostatic screening (*40*) and changes in hydration (*41*).

A model has been reported for regulation of the oligomeric structure of *B. subtilis* EPSPS by ammonium and GLP based on SDS PAGE and sucrose gradient experiments (*14*). In contrast, the present sedimentation equilibrium experiments show that *S. pneumoniae* EPSPS does not appreciably oligomerize up to about 100 μM EPSPS in the presence or absence of various combinations of monovalent cations, S3P, and GLP (Table 3). Although it is likely that ligand-induced changes in solubility of EPSPS may occur at much higher enzyme concentrations than were studied here, the GLP-binding synergy parameters reported here for S3P and monovalent cations on the *S. pneumoniae* EPSPS are neither derived from nor influenced by changes of oligomerization state.

In view of the large "open-closed" tertiary structure change observed in MurA (*34*, *35*) and proposed for EPSPS (*17*), it is attractive to attribute the GLP binding synergy effects of monovalent cations to preferential binding to the ligand-bound "closed" form of EPSPS. The fact that ammonium increases the affinity of both GLP (Figure 3) and S3P (*19*) separately (i.e., decreases K_d and K_m, respectively) suggests the cation binding site does not rely exclusively on direct interaction with one of these ligands. By this token, monovalent cations NH_4^+ and K^+ appear to act as allosteric effectors of substrate and inhibitor binding to *S. pneumoniae* EPSPS. It is noteworthy that the synergistic cation effects (Figure 3) occur at physiologically relevant concentrations of ammonium in bacteria (0.2−12 mM) (*31*, *42*). This raises the question of whether fluctuations in ammonium concentration may regulate biosynthesis of aromatic amino acids through regulation of EPSPS activity. Regardless, it will be important for rational design of antimicrobial inhibitors targeting EPSPS to account for the synergistic effects of both S3P and monovalent cations.

ACKNOWLEDGMENT

We thank Mark Fulston and Anna L. Stefanska for synthesizing the shikimate-3-phosphate.

REFERENCES

1. Haslam, E. (1993) in *Shikimic Acid: Metabolism and Metabolites*, John Wiley, Chickester.
2. Rogers, H. J., Perkins, H. R., and Ward, J. B. (1980) in *Microbial cell walls and membranes*, Chapman & Hall, London.
3. Amrhein, N., and Steinrücken, H. C. (1980) *Biochem. Biophys. Res. Commun. 94*, 1207−1212.
4. Steinrücken, H. C., and Amrhein, N. (1984) *Eur. J. Biochem. 143*, 351−357.
5. Boocock, M. R., and Coggins, J. R. (1983) *FEBS Lett. 154*, 127−133.
6. Anderson, K. S., Sikorski, J. A., and Johnson, K. A. (1988) *Biochemistry 27*, 1604−1610.
7. McDowell, L. M., Klug, C. A., Beusen, D. D., and Schaefer, J. (1996) *Biochemistry 35*, 5395−5403.
8. Merabet, E. K., Walker, M. C., Yuen, H. K., and Sikorski, J. A. (1993) *Biochim. Biophys. Acta 1161*, 272−278.
9. Sammons, R. D., Gruys, K. J., Anderson, K. S., Johnson, K. A., and Sikorski, J. A. (1995) *Biochemistry 34*, 6433−6440.
10. Marzabadi, M. R., Gruys, K. J., Pansegrau, P. D., Walker, M. C., Yuen, H. K., and Sikorski, J. A. (1996) *Biochemistry 35*, 4199−4210.
11. Marzabadi, M. R., Font, J. L., Gruys, K. J., Pansegrau, P. D., and Sikorski, J. A. (1992) *Bioorg. Med. Chem. Lett. 2*, 1435−1440.
12. Shuttleworth, W. A., Hough, C. D., Bertrand, K. P., and Evans, J. N. (1992) *Protein Eng. 5*, 461−466.
13. Padgette, S. R., Re, D. B., Gasser, C. S., Eichholtz, D. A., Frazier, R. B., Hironaka, C. M., Levine, E. B., Shah, D. M., Fraley, R. T., and Kishore, G. M. (1991) *J. Biol. Chem. 266*, 22364−22369.
14. Majumder, K., Selvapandiyan, A., Fattah, F. A., Arora, N., Ahmad, S., and Bhatnagar, R. K. (1995) *Eur. J. Biochem. 229*, 99−106.
15. Sikorski, J. A., and Gruys, K. J. (1997) *Acc. Chem. Res. 30*, 2−8.
16. Ream, J. E., Yuen, H. K., Frazier, R. B., and Sikorski, J. A. (1992) *Biochemistry 31*, 5528−5534.
17. Krekel, F., Oecking, C., Amrhein, N., and Macheroux, P. (1999) *Biochemistry 38*, 8864−8878.
18. Stallings, W. C., Abdel-Meguid, S. S., Lim, L. W., Shieh, H.-S., Dayringer, H. E., Leimgruber, N. K., Stegeman, R. A., Anderson, K. S., Sikorski, J. A., Padgette, S. R., and Kishore, G. M. (1991) *Proc. Natl. Acad. Sci. U.S.A. 88*, 5046−5050.
19. Du, W., Wallis, N. G., Mazzulla, M. J., Chalker, A. F., Zhang, L., Liu, W.-S., Kallender, H., and Payne, D. J. (2000) *Eur. J. Biochem. 267*, 222−227.
20. Fischer, R. S., Rubin, J. L., Gaines, C. G., and Jensen, R. A. (1987) *Arch. Biochem. Biophys. 256*, 325−334.
21. Wiseman, T., Williston, S., Brandts, J. F., and Lin, L.-N. (1989) *Anal. Biochem. 179*, 131−137.
22. Doyle, M. L. (1999) Titration Microcalorimetry In *Current Protocols in Protein Science (Unit 20.4): Titration Microcalorimetry* (Chanda, V., Ed.) John Wiley and Sons, Inc., New York.
23. Pace, C. N., Vajdos, F., Fee, L., Grimsley, G., and Gray, T. (1995) *Protein Sci. 4*, 2411−2423.
24. Doyle, M. L., and Hensley, P. (1997) *Adv. Mol. Cell Biol.* 279−337.
25. Woody, R. W. (1995) *Methods Enzymol. 246*, 34−71.
26. Doyle, M. L., Weber, P. C., and Gill, S. J. (1985) *Biochemistry 24*, 1987−1991.
27. Wyman, J., and Gill, S. J. (1990) *Binding and linkage*, University Science Books, Mill Valley, CA.
28. Di Cera, E. (1995) *Thermodynamic Theory of Site-Specific Binding Processes*, Cambridge University Press, Cambridge.
29. Denbigh, K. (1971) *The principles of chemical equilibrium*, University Press, Cambridge.
30. De Cristofaro, R., Fenton, J. W., II, and Di Cera, E. (1992) *Biochemistry 31*, 1147−1153.
31. Kleiner, D. (1985) *FEMS Microbiol. Rev. 32*, 87−100.
32. Freire, E. (1995) *Annu. Rev. Biophys. Biomol. Struct. 24*, 141−165.
33. Gruys, K. J., Walker, M. C., and Sikorski, J. A. (1992) *Biochemistry 31*, 5534−5544.
34. Schönbrunn, E., Sack, S., Eschenburg, S., Perrakis, A., Krekel, F., Amrhein, N., and Mandelkow, E. (1996) *Structure 4*, 1065−1075.
35. Skarzynski, T., Mistry, A., Wonacott, A., Hutchinson, S. E., Kelly, V. A., and Duncan, K. (1996) *Structure 4*, 1465−1474.
36. Doyle, M. L., Louie, G., Dal Monte, P. R., and Sokoloski, T. D. (1985) *Methods Enzymol. 259*, 183−194.
37. Edgcomb, S. P., and Murphy, K. P. (2000) *Curr. Opin. Biotechnol. 11*, 62−66.
38. Woehl, E., and Dunn, M. F. (1999) *Biochemistry 38*, 7118−7130.
39. Rhee, S., Parris, K. D., Ahmed, S. A., Miles, E. W., and Davies, D. R. (1996) *Biochemistry 35*, 4211−4221.
40. Nørby, J. G., and Esmann, M. (1997) *J. Gen. Physiol. 109*, 555−570.
41. Parsegian, V. A., Rand, R. P., and Rau, D. C. (1995) *Methods Enzymol. 259*, 94.
42. Kung, F.-C., Raymond, J., and Glaser D. A. (1976) *J. Bacteriol. 126*, 1089−1095.
43. Mean activity coefficients of electrolytes as a function of concentration (1995) in *CRC Handbook of Chemistry and Physics* (Lide, D. R., Ed.) pp 5-94−5-98, CRC Press, Inc., Boca Raton, FL.

BI000890V